# Does phenomenological kinetics provide an adequate description of heterogeneous catalytic reactions?

Burcin Temel
*Department of Chemistry and Biochemistry, University of California at Santa Barbara, Santa Barbara, California 93106*

Hakim Meskine and Karsten Reuter
*Fritz-Haber-Institut der Max-Planck-Gesellschaft, Faradayweg 4-6, D-14195 Berlin, Germany*

Matthias Scheffler
*Department of Chemistry and Biochemistry, University of California at Santa Barbara, Santa Barbara, California 93106; Materials Department, University of California at Santa Barbara, Santa Barbara, California 93106; and Fritz-Haber-Institut der Max-Planck-Gesellschaft, Faradayweg 4-6, D-14195 Berlin, Germany*

Horia Metiu
*Department of Chemistry and Biochemistry, University of California at Santa Barbara, Santa Barbara, California 93106 and; Fritz-Haber-Institut der Max-Planck-Gesellschaft, Faradayweg 4-6, D-14195 Berlin, Germany*

(Received 28 November 2006; accepted 26 April 2007; published online 31 May 2007)

Phenomenological kinetics (PK) is widely used in the study of the reaction rates in heterogeneous catalysis, and it is an important aid in reactor design. PK makes simplifying assumptions: It neglects the role of fluctuations, assumes that there is no correlation between the locations of the reactants on the surface, and considers the reacting mixture to be an ideal solution. In this article we test to what extent these assumptions damage the theory. In practice the PK rate equations are used by adjusting the rate constants to fit the results of the experiments. However, there are numerous examples where a mechanism fitted the data and was shown later to be erroneous or where two mutually exclusive mechanisms fitted well the same set of data. Because of this, we compare the PK equations to "computer experiments" that use kinetic Monte Carlo (kMC) simulations. Unlike in real experiments, in kMC the structure of the surface, the reaction mechanism, and the rate constants are known. Therefore, any discrepancy between PK and kMC must be attributed to an intrinsic failure of PK. We find that the results obtained by solving the PK equations and those obtained from kMC, while using the same rate constants and the same reactions, do not agree. Moreover, when we vary the rate constants in the PK model to fit the turnover frequencies produced by kMC, we find that the fit is not adequate and that the rate constants that give the best fit are very different from the rate constants used in kMC. The discrepancy between PK and kMC for the model of CO oxidation used here is surprising since the kMC model contains no lateral interactions that would make the coverage of the reactants spatially inhomogeneous. Nevertheless, such inhomogeneities are created by the interplay between the rate of adsorption, of desorption, and of vacancy creation by the chemical reactions. © *2007 American Institute of Physics*. [DOI: 10.1063/1.2741556]

## I. INTRODUCTION

In recent years it has become possible to analyze the chemical kinetics on solid surfaces by using the kinetic Monte Carlo (kMC) method.[1–4] The input to kMC is a list of the rate constants of all elementary processes that can take place on the surface: adsorption, desorption, diffusion, and chemical reactions. A simulation may start, for example, with a clean surface and with the molecules in the gas phase. The molecules may then adsorb on the surface, diffuse from site to site, and react when they are in the appropriate positions. The results are meaningful if each event is executed with the appropriate rate. This is done by using the rates of all processes possible in a given molecular configuration to construct probabilities for each event that can occur next. Weighted by these probabilities, one event is executed randomly, and, after this execution, the time is advanced appropriately and the probabilities are adjusted to correspond to the new molecular configuration. Then, a new event is executed. Unlike other Monte Carlo procedures, kMC thus provides the evolution of the system out of equilibrium, in real time. When applied to chemical kinetics, kMC provides an efficient numerical method for finding the evolution of concentrations caused by the atomistic kinetic events included in the model, without making further approximations.[5] Since the early conceptual work of Ziff *et al.*[6] kMC has been used to examine various models of CO oxidation,[6–23] which is the reaction of interest in this paper.

Rather than kMC, a practical catalytic research and much of surface science use phenomenological rate equations, in which the reaction rate is proportional to the con-

 

centrations of the reactants. One proposes a mechanism, writes the corresponding rate equations, and varies the rate constants to fit the data. Very often, the fitting is rather good, and this is taken as a confirmation of the proposed mechanism. Due to its usefulness in reactor design, this procedure has reached a high level of sophistication.[24,25] There are, however, many examples in which a given kinetic mechanism fitted the data well, only to fall apart as the data were extended to other temperatures or concentrations, or when it was discovered that reactions not included in the analysis took place in the system. Classic examples are the reactions of halogens with hydrogen whose kinetics was fitted well by a second order equation. Two decades of subsequent work established that, without doubt, this is a complicated chain reaction having more than five steps.[26] For a practical engineer this may not be a problem: Even if the proposed mechanism is erroneous, the equations can be used to design a reactor as long as they fit the data. However, such usage presumes that the equations can be used for conditions for which measurements are not available. As many examples show, such extrapolation is dangerous: If the mechanism is incorrect, the extrapolation could be erroneous even though the equations fitted well a limited set of data. Furthermore, once the data are fitted, the resulting rate constants are used to extract activation energies. If the fit is good, but accidental, the activation energies extracted from the rate constants are meaningless and are a source of confusion.

Why would we doubt the validity of the phenomenological equations, besides possible uncertainties regarding the true reaction mechanism? First, the reaction between two adsorbed molecules, A and B, is proportional to the probability that they are in the right position (e.g., nearest neighbors), not with the product of their coverages. Using the product is a mean-field approximation which assumes a perfect and rapid mixing of the reactants that leads to uniformity in the distribution of reactants on the surface. In most catalytic reactions this may not be the case. The interaction between the adsorbed molecules can lead to segregation into domains containing mostly one kind of molecules. Even when thermodynamics favors a uniform distribution, the kinetics of adsorption, desorption, diffusion, and reaction can create nonuniformity[23] if the time to reach an equilibrium distribution on the surface is longer than the time it takes for kinetics to destroy spatial uniformity.

Another failure of the phenomenological kinetics (PK) equations is displayed by the detailed balance. For a reversible reaction, in which the forward and the backward rates are proportional to the concentrations, the rate equations lead to an equilibrium constant that depends on concentrations. This equilibrium constant is correct only if the reactants and the products form an ideal mixture;[27] i.e., only then do the PK rate equations provide the correct equilibrium.[28,29]

These objections to the PK equations are not new, and possible remedies have been discussed in the literature.[8,25,28–32] Kinetic Monte Carlo simulations do not have any of these flaws. Because they take into account the interactions between the molecules and their diffusion on the surface, the kMC simulations build up the correct spatial distribution of the molecules, and two molecules react only when they are in the proper positions. Since interactions are accounted for correctly, the thermodynamic activity of the reactants and products is automatically taken into account, and if the kMC rate constants are derived properly,[23] there is no conflict with the detailed balance. Since the simulations are stochastic, and each event takes place with the appropriate probability, fluctuations are also treated correctly.

These observations prompted us to undertake the present study, in which we compare the results of kMC simulations to the results obtained by solving the PK rate equations for the same model. We feel that this is more instructive than a comparison of the PK equations to the experiment since in kMC we know with certainty the reaction mechanism and every rate constant. Therefore, any discrepancy between kMC and PK is due to intrinsic shortcomings of the PK theory. In addition, the kMC allows us to understand the cause of the discrepancy since we can examine whether reactant segregation takes place and we can determine the probability that two reactant molecules are nearest neighbors and compare it to the product of the coverages.

To perform this comparison we use the example of the catalytic oxidation of CO by a $RuO_2(110)$ surface, which was examined by kMC in previous work by Reuter and Scheffler.[23] The rate constants have been calculated using transition state theory with activation energies obtained with density-functional theory (DFT).[23] The results of the kMC simulation are in good agreement with experiment.[33] Since we use the kMC simulations as a computer experiment, the agreement with experiment is not even really necessary; it is, however, reassuring to know that we do not study a model whose parameters are far from reality.

Section II reviews briefly the properties of the surface and the kMC model, and presents the rate equations used in the PK calculations. Section III compares the dependence of the steady-state surface coverage on the partial pressures of CO and $O_2$, calculated with kMC and PK. The qualitative description provided by PK for this dependence is similar to that obtained in kMC. The main result is that the $CO_2$ formation is rapid only in a certain range of CO and $O_2$ partial pressures. Outside this range, the surface is covered almost completely by one of the components, and the reaction is very slow. While PK is qualitatively correct, it is quantitatively erroneous: The pressures at which the activity of the catalyst is highest in the PK calculations are fairly different from those given by kMC, and under other pressure conditions the PK activity differs from the kMC activity by up to a few orders of magnitude. In Sec. IV we take the view that the kMC produces "experimental data" and then vary the rate constants in the PK theory to get the best fit of these data. If the PK theory were correct, the fit would be good and the rate constants giving the best fit would be close to those used in the kMC simulation. We find that this is not the case: The fit is fairly poor and the rate constants giving the best fit are very different from those used in the kMC simulation (which are the correct rate constants).

The kMC simulations provide the positions of the atoms on the surface during the reaction. Therefore, we can calculate both the probability that CO and O are neighbors on the lattice and the product of their coverages. We find, in Sec. V,

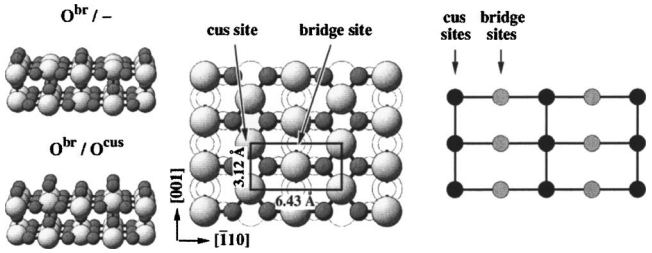


FIG. 1. Central panel: Top view of the $RuO_2$ (110) surface showing the two prominent adsorption sites (br and cus). When focusing on these two sites, the surface can be coarse grained to the lattice model shown schematically to the right. Additionally shown are two perspective views in the left panels, exemplifying what the atomic structure of the surface looks like if all bridge sites are occupied with oxygen atoms and the cus sites remain empty (the yellow $O^{br}$/– "phase" in Figs. 2 and 3, top left panel), or if oxygen atoms occupy both site types (the red $O^{br}/O^{cus}$ phase in Figs. 2 and 3, bottom left panel). Ru=light, large spheres; O=dark, small spheres. Atoms lying in deeper layers have been whitened in the top view for clarity.

that these two quantities differ from each other (while the mean-field ideal-mixture approximation implicit in PK assumes them to be the same). We show that this difference arises because the rates of deposition and removal of CO and $O_2$ on the surface create a substantial concentration inhomogeneity in spite of the fact that the species are allowed to diffuse on the surface.

## II. THE MODEL

As we have already mentioned, many publications[6–23] have presented kMC simulations of catalytic CO oxidation by using a variety of models. We examine here the kinetics of a model of CO oxidation by a "Ru catalyst" which has been extensively studied theoretically by Reuter *et al.*[21–23,34–38] These calculations have found that in a catalytically most active state and in the case of the Ru(0001) single-crystal surface, the catalyst is, in fact, a $RuO_2$(110) film that forms during the oxidation reaction. These findings are in agreement with the experimental results.[39–55] The calculations also show that the (110) face of $RuO_2$ has two distinct adsorption sites for O or CO: the bridge (br) site where the adsorbate binds to two Ru atoms and the coordinatively unsaturated (cus) site where the adsorbate is on top of a Ru atom (see Fig. 1). Each rectangular $(1\times1)$ surface unit cell has one br and one cus site. Both molecules can adsorb on either the bridge or the cus sites; $O_2$ binds dissociatively and CO binds without dissociation. $CO_2$ does not bind to the surface and leaves it as soon as it is formed.

The kinetic Monte Carlo calculations are performed on the lattice model shown in the right-hand panel in Fig. 1, where each site corresponds to a surface area $A_s=10.03$ Å$^2$. All simulations have been conducted on a system with $20\times20$ surface sites (200 br and 200 cus sites) and periodic boundary conditions. Test runs for a $40\times40$ system led to identical results for the quantities reported here.

The simulation takes into account the following events: The adsorption-desorption processes are

$$\mathrm{CO}^{\mathrm{br}} \underset{k_{-1}}{\overset{k_1}{\rightleftarrows}} \mathrm{CO}^{\mathrm{gas}} + V^{\mathrm{br}}, \quad E_1 = 1.6\ \mathrm{eV}, \tag{1}$$

$$\mathrm{CO}^{\mathrm{cus}} \underset{k_{-2}}{\overset{k_2}{\rightleftarrows}} \mathrm{CO}^{\mathrm{gas}} + V^{\mathrm{cus}}, \quad E_2 = 1.3\ \mathrm{eV}, \tag{2}$$

$$2\mathrm{O}^{\mathrm{br}} \underset{k_{-3}}{\overset{k_3}{\rightleftarrows}} \mathrm{O}_2^{\mathrm{gas}} + 2V^{\mathrm{br}}, \quad E_3 = 4.6\ \mathrm{eV}, \tag{3}$$

$$2\mathrm{O}^{\mathrm{cus}} \underset{k_{-4}}{\overset{k_4}{\rightleftarrows}} \mathrm{O}_2^{\mathrm{gas}} + 2V^{\mathrm{cus}}, \quad E_4 = 2.0\ \mathrm{eV}, \tag{4}$$

$$\mathrm{O}^{\mathrm{br}} + \mathrm{O}^{\mathrm{cus}} \underset{k_{-5}}{\overset{k_5}{\rightleftarrows}} \mathrm{O}_2^{\mathrm{gas}} + V^{\mathrm{br}} + V^{\mathrm{cus}}, \quad E_5 = 3.3\ \mathrm{eV}. \tag{5}$$

Here, $V$ denotes a vacant lattice site and $E_i$ are the energy barriers to desorption calculated with DFT.

In addition, the model includes the following reactions among the adsorbates:

$$\mathrm{CO}^{\mathrm{br}} + \mathrm{O}^{\mathrm{cus}} \xrightarrow{k_6} \mathrm{CO}_2 + V^{\mathrm{br}} + V^{\mathrm{cus}}, \quad E_6 = 0.8\ \mathrm{eV}, \tag{6}$$

$$\mathrm{CO}^{\mathrm{br}} + \mathrm{O}^{\mathrm{br}} \xrightarrow{k_7} \mathrm{CO}_2 + 2V^{\mathrm{br}}, \quad E_7 = 1.5\ \mathrm{eV}, \tag{7}$$

$$\mathrm{CO}^{\mathrm{cus}} + \mathrm{O}^{\mathrm{cus}} \xrightarrow{k_8} \mathrm{CO}_2 + 2V^{\mathrm{cus}}, \quad E_8 = 0.9\ \mathrm{eV}, \tag{8}$$

$$\mathrm{CO}^{\mathrm{cus}} + \mathrm{O}^{\mathrm{br}} \xrightarrow{k_9} \mathrm{CO}_2 + V^{\mathrm{cus}} + V^{\mathrm{br}}, \quad E_9 = 1.2\ \mathrm{eV}. \tag{9}$$

Here, $E_i$ are the activation energies, again calculated with DFT.[23] The DFT calculations[23] find that $CO_2$ binds only very weakly to the surface, so that the reverse processes in Eqs. (6)–(9) are not considered.

The kMC program also includes the diffusion of the species on the surface. The site-to-site hopping rates were determined[23] by using DFT to calculate the activation energy and transition state theory to determine the hopping rates. The reaction rates are such that at high gas pressures, the adsorption rate is much higher than the rate of vacancy creation in the oxygen layer (by either desorption or reaction). Because of this, at high pressures most surface sites are occupied and diffusion becomes unimportant. Using the equations provided in the Appendix, the energies $E_i$ (for given gas-phase conditions, i.e., temperature and partial pressure) determine the rates $k_{\mathrm{kMC},i}$ with which the individual events are executed in the kMC simulations.

In summary, the kMC model takes into account the dissociative adsorption of $O_2$ resulting in three possible postadsorption states (two O atoms in neighboring cus sites, two O atoms in neighboring br sites, or two O atoms, one in a br site and one in a neighboring cus site); the associative desorption of $O_2$ from each of the three configurations of the O atoms; the adsorption of CO in cus or br sites; the desorption of CO from cus or br sites; the reaction of CO with O from four different initial states (O in cus reacting with CO in cus, O in cus with CO in br, O in br with CO in br, and O in br with CO in cus); and the hops of O and CO from a site to the nearest site (for all possible site combinations). The rates for all these processes are calculated by using DFT to determine the energy barriers and transition state theory to calculate the rate constants. The sticking coefficients of CO and $O_2$ are

equal to 1.[23] This is the most comprehensive model of CO oxidation proposed to date, in which every kinetic assumption (binding sites, rates, and structures) is based on DFT. The model, with no adjustable parameters, is in good agreement with the experiments.[23] For testing the phenomenology it is not essential that the model represents precisely a specific system, but it is important to use a model that represents a realistic situation; one would not want to examine phenomenological kinetics under conditions that are never met in practice.

The kMC calculations are performed by using the standard rejection-free algorithm[1–4] and by keeping constant the temperature, the partial pressures of CO and $O_2$, and the total pressure; this means that it is assumed that $CO_2$ is removed efficiently from the reacting system and the heat of reaction is quickly dissipated away. The same assumptions are made when writing the PK equations displayed below. Since our purpose is to compare the kMC results to the PK ones, it is essential that we use the same conditions in both programs.

Considering the processes described in Eqs. (1)–(9), the corresponding PK rate equations for the coverages of the various adsorbed species are

$$\frac{d\theta CO^{br}(t)}{dt} = k_{-1}\theta V^{br}(t) - k_1\theta CO^{br}(t) - k_6\theta O^{cus}(t)\theta CO^{br}(t) - k_7\theta O^{br}(t)\theta CO^{br}(t), \tag{10}$$

$$\frac{d\theta CO^{cus}(t)}{dt} = k_{-2}\theta V^{cus}(t) - k_2\theta CO^{cus}(t) - k_8\theta O^{cus}(t)\theta CO^{cus}(t) - k_9\theta O^{br}(t)\theta CO^{cus}(t), \tag{11}$$

$$\frac{d\theta O^{br}(t)}{dt} = 2k_{-3}\theta V^{br}(t)^2 - 2k_3\theta O^{br}(t)^2 + k_{-5}\theta V^{br}(t)\theta V^{cus}(t) - k_5\theta O^{br}(t)\theta O^{cus}(t) - k_7\theta CO^{br}(t)\theta O^{br}(t) - k_9\theta CO^{cus}(t)\theta O^{br}(t), \tag{12}$$

$$\frac{d\theta O^{cus}(t)}{dt} = 2k_{-4}\theta V^{cus}(t)^2 - 2k_4\theta O^{cus}(t)^2 + k_{-5}\theta V^{br}(t)\theta V^{cus}(t) - k_5\theta O^{br}(t)\theta O^{cus}(t) - k_6\theta CO^{br}(t)\theta O^{cus}(t) - k_8\theta CO^{cus}(t)\theta O^{cus}(t). \tag{13}$$

Because the system has two sublattices, formed by cus and br sites, the definition of coverage can be an endless source of confusion. In the above equations (and everywhere where the symbol $\theta$ is used), the coverage refers to the sublattice sites. Thus, the symbol $\theta A^x$ denotes the total number of molecules A in all sites $x$ divided by the total number $N^x$ of $x$ sites on the surface. For example, $\theta CO^{cus}$ is the number of CO molecules on the cus sites divided by the total number of cus sites. In the model, a site is either occupied by a CO molecule or a O atom, or it is empty; multiple site occupation is not allowed. The factor of 2 in some of the terms in Eq. (12) is present because the adsorption or desorption of one $O_2$ molecule creates or removes two oxygen atoms on the br sites. The factors of 2 in Eq. (13) are introduced for a similar reason.

TABLE I. Rate constants ($s^{-1}$) for the two gas-phase conditions discussed frequently in the text: $T=600$ K ($p_{CO}=7$ atm and $p_{O_2}=1$ atm) and $T=350$ K ($p_{CO}=4\times10^{-10}$ atm and $p_{O_2}=1\times10^{-10}$ atm).

| Process | $k_i$ (600 K) | $k_i$ (350 K) |
|---|---|---|
| $CO^{br}$ adsorption | $7.2\times10^{8}$ | $5.0\times10^{-2}$ |
| $CO^{cus}$ adsorption | $7.2\times10^{8}$ | $5.0\times10^{-2}$ |
| $O^{br}+O^{br}$ adsorption | $9.7\times10^{7}$ | $1.0\times10^{-2}$ |
| $O^{cus}+O^{cus}$ adsorption | $9.7\times10^{7}$ | $1.0\times10^{-2}$ |
| $O^{br}+O^{cus}$ adsorption | $9.7\times10^{7}$ | $1.0\times10^{-2}$ |
| $CO^{br}$ desorption | $2.8\times10^{4}$ | $1.4\times10^{-6}$ |
| $CO^{cus}$ desorption | $9.2\times10^{6}$ | $2.9\times10^{-2}$ |
| $O^{br}+O^{br}$ desorption | $4.1\times10^{-21}$ | $2.0\times10^{-49}$ |
| $O^{cus}+O^{cus}$ desorption | $2.8\times10^{1}$ | $5.5\times10^{-12}$ |
| $O^{br}+O^{cus}$ desorption | $3.4\times10^{-10}$ | $1.1\times10^{-30}$ |
| $CO^{br}+O^{cus}\rightarrow CO_2$ | $1.2\times10^{6}$ | $1.1\times10^{1}$ |
| $CO^{br}+O^{br}\rightarrow CO_2$ | 1.6 | $9.2\times10^{-10}$ |
| $CO^{cus}+O^{cus}\rightarrow CO_2$ | $1.7\times10^{5}$ | 0.4 |
| $CO^{cus}+O^{br}\rightarrow CO_2$ | $5.2\times10^{2}$ | $1.9\times10^{-5}$ |

On purpose, the phenomenological model does not include the diffusion of the various species on the surface. This approximation, which is most common, assumes that the role of diffusion is to create a perfect mixing of the species on the surface, which justifies the use of the products of surface concentrations (coverages) in the rate equation. In order to make contact with common practice in the PK theory, we therefore do not explicitly consider diffusion in the rate equations, although it would be technically easy to do so.

By using the conservation conditions

$$\theta V^{br}(t) = 1 - \theta CO^{br}(t) - \theta O^{br}(t), \tag{14}$$

$$\theta V^{cus}(t) = 1 - \theta CO^{cus}(t) - \theta O^{cus}(t), \tag{15}$$

we eliminate the vacancy "coverages," $\theta V^{cus}$ and $\theta V^{br}$, from the rate equations. After this elimination, the four differential equations describe the evolution of $\theta CO^{cus}$, $\theta CO^{br}$, $\theta O^{cus}$, and $\theta O^{br}$. These coupled, nonlinear, differential equations are solved numerically, with MATHEMATICA, by using the function NDSolve with a method that solves stiff equations.

Finally, we comment on the relationship between the rate constants used in PK and those used in kMC. Let us assume that we are interested in the reaction of $A^x+B^y$, where A and B could be O, CO, or a vacancy $V$ (when the "reaction" is an adsorption) and $x$ and $y$ are the sites where the species are located (i.e., cus or br). In kMC the contribution of this reaction to the rate of formation of the molecule AB (at a given moment in time) is

$$\text{rate}(A^x,B^x) = k_{kMC}(A^x,B^y)N_2(A^x,B^y). \tag{16}$$

Here, $k_{kMC}(A^x,B^y)$ is the rate constant for the reaction of $A^x$ with $B^y$ (the values of these rate constants for certain temperature and pressure conditions are given in Table I). We note that sometimes in the kMC literature, $k_{kMC}(A^x,B^y)$ is

called the rate of reaction, but we will not use this nomenclature here. In addition, in kMC and the phenomenological theory the adsorption rate of compound A is proportional to the partial pressure of A. We have included the partial pressure of CO or $O_2$ in the rate constant for adsorption because all the calculations are done at a constant pressure. This is not always the custom in chemical kinetics which often uses rate expressions in which the partial pressure is displayed explicitly.

$N_2(A^x,B^y)$ is the number of A-B pairs that are next-neighbors, with A on site $x$ and B on site $y$. Equation (16) thus gives the number of AB molecules produced per unit time by the reaction $A^x+B^y$. The phenomenological theory calculates the rate by replacing $N_2(A^x,B^y)$ with the mean-field approximation

$$N_2(A^x,B^y) \rightarrow \frac{N}{2}\frac{N_1(A^x)}{N^x}\frac{N_1(B^y)}{N^y} = \frac{N}{2}\theta A^x \theta B^y, \tag{17}$$

i.e., it replaces $N_2(A^x,B^y)$ by the probability to find species A at sites $x$ times the probability to find species B at sites $y$ times the total number of $x$-$y$ site pairs. Here, $N_1(A^x)$ is the number of molecules A on the $x$ sublattice, $N_1(B^y)$ is the number of molecules B on the $y$ sublattice, and $N=N^{cus}+N^{br}$ is the total number of sites on the lattice. $\theta A^x$ and $\theta A^y$ are the coverages defined earlier. Using this replacement in Eq. (17) tells us that the contribution of the reaction $A^x+B^y$ to the production of AB is given by $k_{kMC}(A^x,B^y)\times(N/2)\theta A^x \theta B^y$ in the phenomenological theory.

We are interested here in the turnover frequency (TOF) for $CO_2$ production which is the number of $CO_2$ molecules produced jointly by all reactions per unit time divided by the number of lattice sites $N$. In PK this quantity is calculated, after solving the differential equations, from

$$\begin{aligned} \mathrm{TOF}(CO_2,t) = \tfrac{1}{2}\{&k_6\theta CO^{br}(t)\theta O^{cus}(t) + k_7\theta CO^{br}(t)\theta O^{br}(t) \\ &+ k_8\theta CO^{cus}(t)\theta O^{cus}(t) \\ &+ k_9\theta CO^{cus}(t)\theta O^{br}(t)\}. \end{aligned} \tag{18}$$

In principle, phenomenological theory could replace the mean-field assumption [Eq. (17)] with a better approximation that takes into account some of the effects of statistical correlations. In practice, this is, however, rarely done, and we are not aware of proposed assumptions that have been proven correct.

## III. THE DEPENDENCE OF THE STEADY-STATE COVERAGES AND OF THE $CO_2$ PRODUCTION RATE ON THE $O_2$ AND CO PARTIAL PRESSURES

The dependence of the TOF for $CO_2$ production on the gas-phase conditions is conveniently described by a kinetic phase diagram, introduced in the previous work,[23] shown in the left panels of Figs. 2 and 3. For a fixed temperature and every pair of partial pressures $(p_{CO},p_{O_2})$ we represent the composition of the surface by a color coded point. For example, at the partial pressures corresponding to the red region more than 90% of the lattice sites are occupied by oxygen atoms. Because there is little CO on the surface, very little $CO_2$ is produced at the pressures corresponding to this

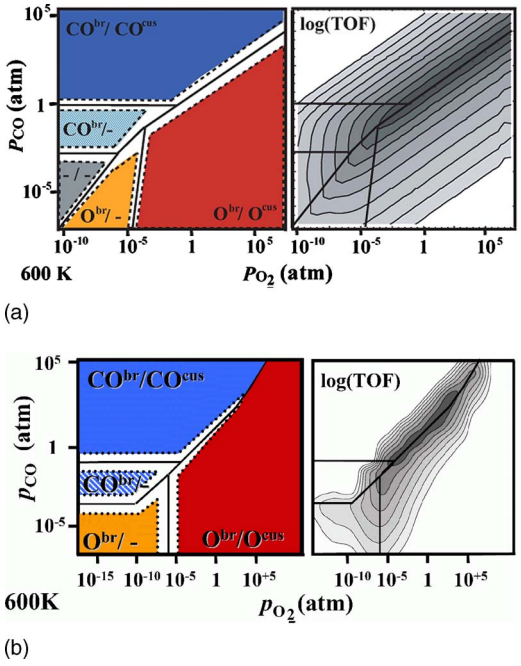


FIG. 2. (Color online) (a) Left panel: A schematic representation of the steady-state coverages obtained by PK, employing the kMC rate constants (Table I), at 600 K, as a function of the partial pressures of CO and $O_2$. In all regions that are not white, the average site population is dominated (>90%) by one species, i.e., either O or CO, or empty sites (−). The labels correspondingly characterize the surface populations by indicating this majority species at the br and at the cus sites. For example, in the blue region ($CO^{br}/CO^{cus}$) more than 90% of the br sites and of the cus sites are occupied by CO molecules. Right panel: A contour map of the turnover frequency (TOF) of $CO_2$ production as a function of the partial pressures. The TOF values increase one order of magnitude from one contour to another, and higher values have darker shading. The white region corresponds to TOF values smaller than $10^{11}$ $cm^{-2}$ $s^{-1}$. (b) Diagrams equivalent to those shown in (a), now obtained by kMC simulations at 600 K. Left panel: Schematic representation of the steady-state coverages. Right panel: Contour map of the TOF for $CO_2$ production. The same contour shading is employed as in (a); i.e., the white areas have a TOF$<10^{11}$ $cm^{-2}$ $s^{-1}$, and each increasing gray level represents one order of magnitude higher activity.

region of the diagram. At the pressures corresponding to the blue region, more than 90% of the sites are occupied by CO molecules; now, the small amount of oxygen on the surface makes CO oxidation slow. Thus, for most partial pressures one of the reactants is present on the surface in very small amounts, which leads to low conversion rates. The points where both components are present on the surface in appreciable amounts and where $CO_2$ is produced with a significant rate are shown in white.

The panels in the right-hand side of Figs. 2 and 3 show contour maps of the TOF for $CO_2$ production, again as a function of the partial pressures of the reactants and of the selected temperatures. The straight heavy lines in the picture show the borders between the various regions in the "kinetic phase diagram." It is intriguing to see how sharply the rate increases, as the pressures at which both components are present on the surface are approached (the rate increases by one order of magnitude from one contour to another).

The topology of the kinetic phase diagrams and contour maps generated by kMC and PK is similar. Both methods predict the existence of different "phases" on the surface and the fact that the reaction is rapid only for a relatively narrow

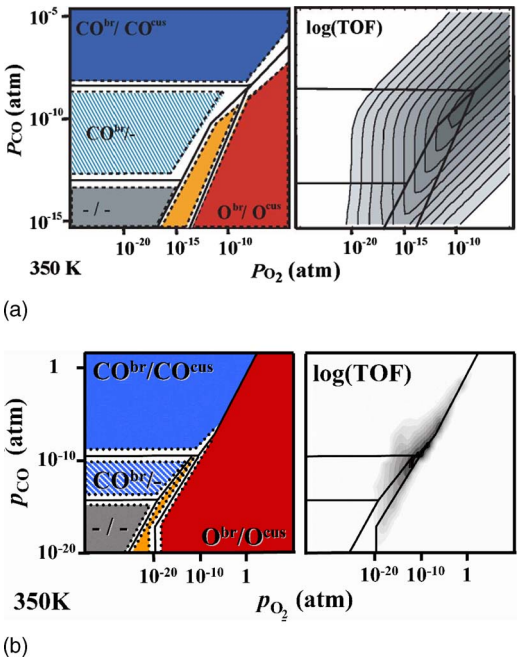


FIG. 3. (Color online) (a) The same information as in Fig. 2(a) for calculations performed with PK at 350 K. At this lower temperature, the TOFs for $CO_2$ production are significantly lower. The white region in the contour plot corresponds now to an activity of less than $10^3$ cm$^{-2}$ s$^{-1}$, and each increasing gray level represents again one order of magnitude higher activity. (b) The same information as in (a) for calculations performed with kMC at 350 K. At this lower temperature, the TOFs for $CO_2$ production are significantly lower. Just as in (a), the white region in the contour plot corresponds now to an activity of less than $10^3$ cm$^{-2}$ s$^{-1}$, and each increasing gray level represents again one order of magnitude higher activity.

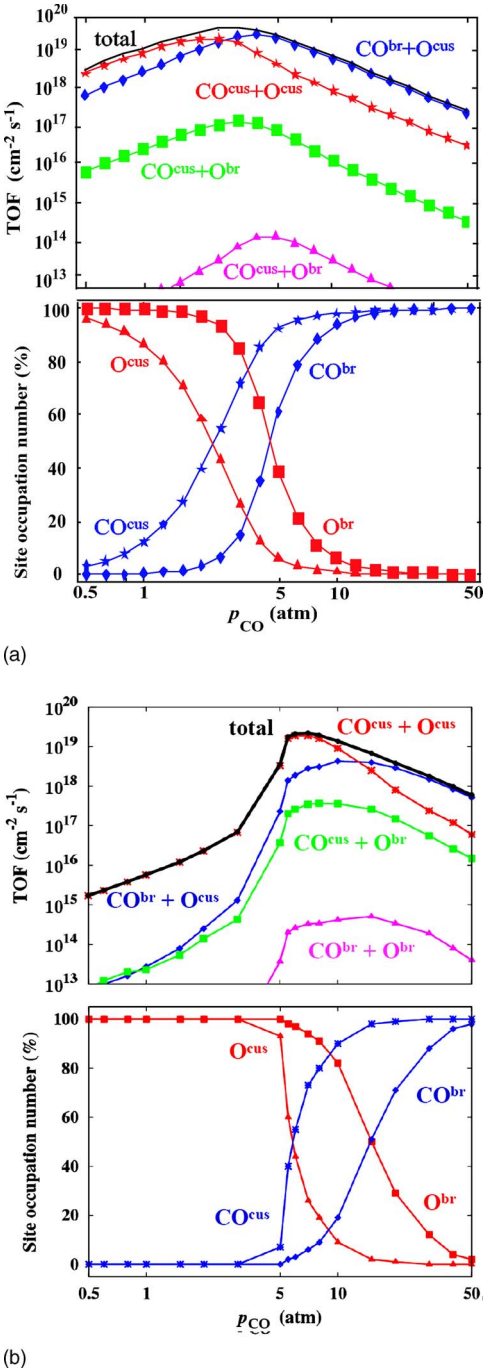


FIG. 4. (Color online) (a) Dependence of the TOF (upper panel) and site occupations (lower panel) obtained with PK employing the kMC rate constants, $T$=600 K and $p_{O_2}$=1 atm. Shown in the upper panel is the dependence of the total TOF, as well as the contribution of the four different reaction mechanisms. The maximum TOF is obtained at $p_{CO}$=3 atm. The lower panel shows the average occupation of the br and cus sites by O or CO. (b) The same information as in (a), but obtained by kMC. Upper panel: The TOF as a function of the CO pressure. The maximum TOF is reached at $p_{CO}$=7 atm. Lower panel: Average site occupation as a function of CO pressure.

range of partial pressures. There are, however, quantitative differences. For example, the region where the catalyst is active is much broader in the PK calculations. These quantitative differences between kMC and PK are better displayed by making one-dimensional graphs along constant-pressure cuts through the "kinetic phase diagram." Figure 4(a) shows the dependence of the steady-state TOF given by PK. The temperature is fixed at 600 K, the oxygen partial pressure is 1 atm, and $p_{CO}$ is varied over a wide range. The figure gives the TOF for total $CO_2$ production (by all reactions) and also the contribution to $CO_2$ production from each of the four reactions taking place on the surface. The TOF peaks sharply (the logarithmic scale flattens the peak) as $p_{CO}$ is varied across the white region of the phase diagram. At higher CO pressures, the main contribution to $CO_2$ formation comes from the reaction $CO^{br}+O^{cus}$, followed by $CO^{cus}+O^{cus}$. At lower pressures the $CO^{cus}+O^{cus}$ is more active than $CO^{br}+O^{cus}$.

Among the four reactions, the rate constant for the $CO^{br}+O^{cus}$ reaction is the largest, and at 600 K it is equal to $1.2\times10^6$ s$^{-1}$. The rate constant for $CO^{cus}+O^{cus}$ is substantially smaller ($0.2\times10^6$ s$^{-1}$) but still exceeds by several orders of magnitude the remaining rate constants (see Table I). If one assumes (as is fairly common practice) that the rate constants alone determine the importance of a reaction, one would falsely conclude that the $CO^{br}+O^{cus}$ reaction is the most important at all CO pressures. However, the steady-state rate is a product of the rate constant with the steady-state coverages, and this must be taken into account when determining which reaction is most important. The results presented in Fig. 4(a) show that in the low pressure range, the product of $\theta CO^{cus}\times\theta O^{cus}$ must be larger than $\theta CO^{br}\times\theta O^{cus}$, and this makes the rate of $CO^{cus}+O^{cus}$ higher, in spite of having the smaller rate constant. At smaller CO pres-

TABLE II. Comparison of the steady-state turnover frequencies (TOFs) due to the four different reaction mechanisms as obtained by PK and kMC (in both cases using the kMC rate constant $k_i$, Table I). The TOFs give $CO_2$ production per s per $cm^2$. Shown are the data for gas-phase conditions corresponding to the peak catalytic activity in Fig. 4(b) ($T$=600 K, $p_{CO}$ =7 atm, and $p_{O_2}$=1 atm).

| Reaction mechanism ($T$=600 K) | PK ($cm^{-2}\,s^{-1}$) | kMC ($cm^{-2}\,s^{-1}$) |
|---|---|---|
| $CO^{br}+O^{br}$ | $1\times10^{14}$ | $1\times10^{14}$ |
| $CO^{cus}+O^{cus}$ | $20\,670\times10^{14}$ | $188\,760\times10^{14}$ |
| $CO^{cus}+O^{br}$ | $390\times10^{14}$ | $3520\times10^{14}$ |
| $CO^{br}+O^{cus}$ | $124\,860\times10^{14}$ | $27\,720\times10^{14}$ |
| Total TOF | $145\,921\times10^{14}$ | $220\,001\times10^{14}$ |

sures, there is thus more $CO^{cus}$ on the surface than $CO^{br}$. In general, this steady-state CO coverage on a given site is a result of the interplay between all the processes in the system. However, in the present case, it is predominantly due to the significantly stronger bonding of oxygen at the br sites, which are then blocked for CO adsorption.

Of greater interest to the present work is the difference between the behaviors predicted by PK and kMC. The kMC results, for $T$=600 K and $p_{O_2}$=1 atm, are shown in Fig. 4(b). We see similarities between the PK and kMC results: Both predict that at high CO pressures $CO^{br}+O^{cus}$ is more productive, followed by $CO^{cus}+O^{cus}$, and that at lower CO pressures this situation is reversed. The evolution of the steady-state coverages with the CO pressure in Figs. 4(a) and 4(b) are also very similar. Despite these similarities, there are quantitative differences (see Table II). The peak in the reaction rates is narrower in kMC, and the evolution of the rate (as the CO pressure is varied) is more abrupt. The highest rate in kMC is that of the reaction $CO^{cus}+O^{cus}$ ($1.9\times10^{19}$ $cm^2\,s^{-1}$) at $p_{CO}$=7 atm, while in PK the rate of this reaction is only $2.1\times10^{18}$ $cm^2\,s^{-1}$ at this pressure. Moreover, under these conditions the fastest reaction in PK is $CO^{br}+O^{cus}$ with a rate of $1.2\times10^{19}$ $cm^2\,s^{-1}$, which is very different from the corresponding kMC rate of $2.8\times10^{18}$ $cm^2\,s^{-1}$. Thus, not only do the rates obtained in PK differ significantly from the kMC ones, but even the dominant reaction is incorrectly identified by PK. There is also a discrepancy in the prediction of the gas-phase conditions for which the highest TOF is obtained: kMC predicts that at $T$ =600 K and $p_{O_2}$=1 atm one should use $p_{CO}$=7 atm, while PK recommends $p_{CO}$=3 atm.

Similar remarks can be made about the results presented in Figs. 5(a) and 5(b), for $T$=350 K and $p_{O_2}=10^{-10}$ atm, for PK and kMC, respectively. The corresponding peak rates at $p_{CO}=4\times10^{-10}$ atm are listed in Table III. For this very low pressure condition the assumption of a random distribution of the adsorbates is apparently better fulfilled. Now PK describes correctly that the clearly dominant reaction is that of $CO^{cus}+O^{br}$.

## IV. THE BEST FIT OF THE KMC "DATA" BY THE PK EQUATIONS

We have already mentioned that we consider the kMC results to be "computer experiments" against which the results of the PK theory can be judged. Here, we pretend that, like in a real experiment, we do not know the rate constants and determine them by adjusting the rate constants in the PK theory so that the TOF calculated by PK fits best the kMC results. More precisely, we model the common situation that the rate constants for adsorption and desorption are believed to be known from independent experiments. These rate constants are therefore set equal to the values used in kMC, and the fitting is restricted to the rate constants of the four reaction processes.

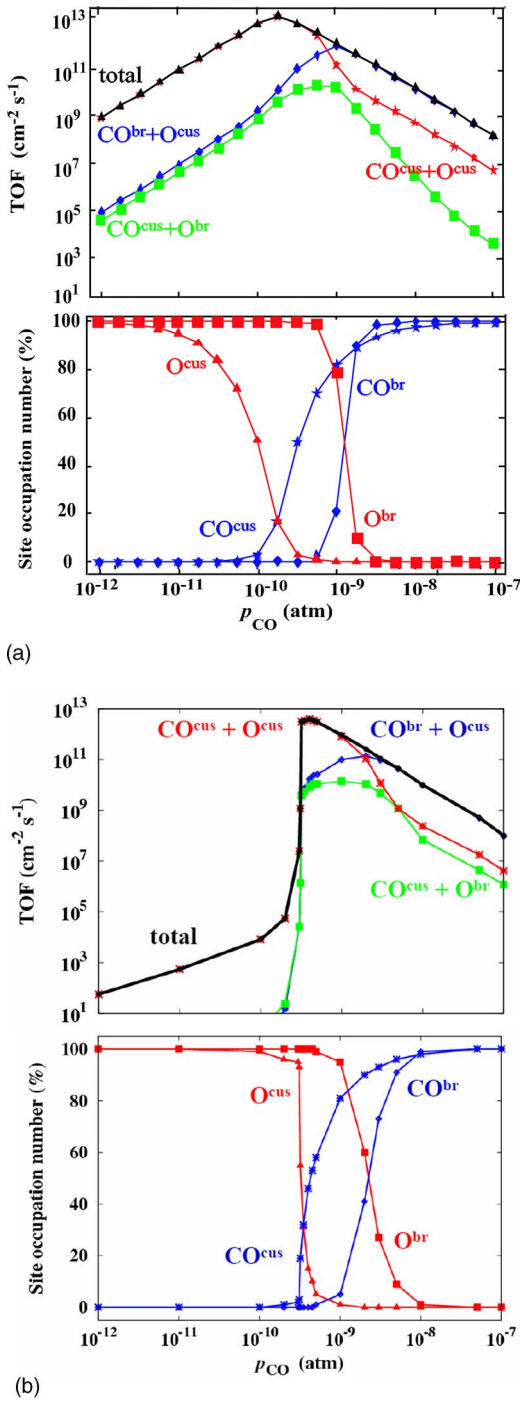


FIG. 5. (Color online) (a) The same information as in Fig. 4(a) for calculations performed with PK at 350 K and $p_{O_2}=1\times10^{-10}$ atm. The maximum TOF is reached at $p_{CO}=2\times10^{-10}$ atm. (b) The same information as in (b) for calculations performed with kMC at 350 K and $p_{O_2}=1\times10^{-10}$ atm. The maximum TOF is reached at $p_{CO}=4\times10^{-10}$ atm.

TABLE III. Comparison of the steady-state turnover frequencies (TOFs) due to the four different reaction mechanisms as obtained by PK and kMC (in both cases using the kMC rate constants $k_i$, Table I). The TOFs give $CO_2$ production per s per $cm^2$. Shown are the data for gas-phase conditions corresponding to the peak catalytic activity in Fig. 5(b) ($T=350$ K, $p_{CO}=4\times10^{-10}$ atm, and $p_{O_2}=1\times10^{-10}$ atm).

| Reaction mechanism ($T=350$ K) | PK ($cm^{-2}\,s^{-1}$) | kMC ($cm^{-2}\,s^{-1}$) |
|---|---|---|
| $CO^{br}+O^{br}$ | 0 | 0 |
| $CO^{cus}+O^{cus}$ | $1850\times10^9$ | $3976\times10^9$ |
| $CO^{cus}+O^{br}$ | $6\times10^9$ | $8\times10^9$ |
| $CO^{br}+O^{cus}$ | $60\times10^9$ | $16\times10^9$ |
| Total TOF | $1916\times10^9$ | $4000\times10^9$ |

We perform this analysis for two kinds of kMC data. In one we fit the evolution of the TOF from the time when the reaction starts to the time when the TOF reaches the steady state for fixed partial pressures, temperature, and initial coverage. In the other, we fit the dependence of the steady-state TOF on the partial pressure of CO, while the temperature, the partial pressure of oxygen, and the initial coverages are all kept constant.

In the first type of fit we "measure" the TOF for $CO_2$ production, $R_{kMC}(t_i)$, as a function of the time $t_i$ for given initial coverages, temperatures, and partial pressures (and averaging over kMC runs with different random number seeds). Then, we define the least-squares error function

$$e(k_6,k_7,k_8,k_9)=\sum_{i=1}^{N}\{R_{kMC}(t_i)-R_{PK}(t_i,k_6,k_7,k_8,k_9)\}^2, \tag{19}$$

where $R_{PK}(t_i)$ is the TOF given by the PK method at the time $t_i$ at which the kMC measurements are made. We vary the rate constants $k_6$, $k_7$, $k_8$, and $k_9$ in $R_{PK}$ to minimize $e(k_6,k_7,k_8,k_9)$. The minimization of $e$ is performed in MATHEMATICA by using the function Minimize. We have experimented with a variety of initial guesses for the iterative minimization and with various constraints on a reasonable range over which the rate constants are varied, to make sure (as far as possible) that we did find the absolute minimum.

In Fig. 6(a) we show the evolution of the $CO_2$ turnover frequencies with time, calculated with PK and with kMC, where we first used the same (kMC) rate constants in both approaches. The conditions are $T=350$ K, $p_{O_2}=1\times10^{-10}$ atm, and $p_{CO}=4\times10^{-10}$ atm, i.e., gas-phase conditions which correspond to the peak catalytic activity in Fig. 5(b). In the initial state all bridge sites on the surface are occupied by oxygen atoms and all cus sites are free. This is the $O^{br}$/– phase, which is the standard surface termination produced after annealing in ultrahigh vacuum. The PK results differ from the kMC ones, but not dramatically. We then adjust $k_6,\ldots,k_9$ until PK gives the best fit to the kMC results. The best fit is shown by the dashed line, and it is quite satisfactory. However, the values of $k_6,\ldots,k_9$ that give the best fit are quite different from the ones used in kMC (see Table IV).

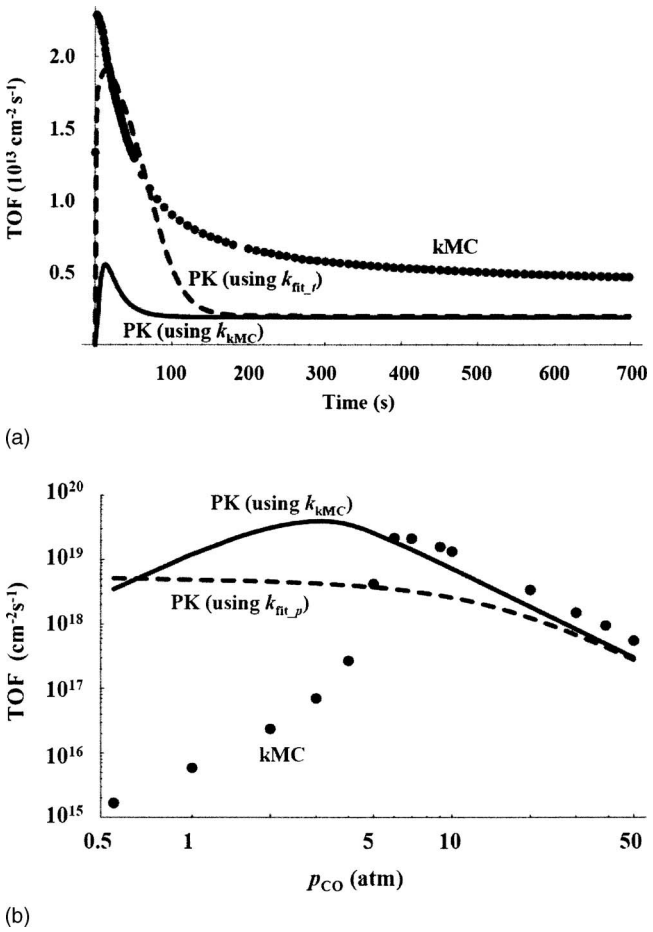


FIG. 6. (a) The evolution of the TOF frequency for $CO_2$ production as a function of time. The solid line gives the turnover frequencies obtained by PK using the kMC rate constants. The circles show the TOF evolution given by kMC. The dashed line represents the TOF evolution given by PK when the reaction rate constants $k_i$ ($i=6,7,8,9$) are adjusted to yield the best fit to the kMC data (Table IV). The gas-phase conditions correspond to the peak catalytic activity in Fig. 5(b), i.e., $T=350$ K, $p_{O_2}=1\times10^{-10}$ atm, and $p_{CO}=4\times10^{-10}$ atm. Note that at the maximum time shown (350 s), the steady state has not yet been reached. The corresponding steady-state TOFs are listed in Table III. (b) The dependence of the steady-state TOF for $CO_2$ production as a function of the CO partial pressure at $T=600$ K and $p_{O_2}=1$ atm. The solid line gives the turnover frequencies obtained by PK using the kMC rate constants. The circles show the TOFs given by kMC. The dashed line represents the TOFs given by PK when the reaction rate constants $k_i$ ($i=6,7,8,9$) are adjusted to yield the best fit to the kMC data (Table IV).

The discrepancy is rather large, but it is not as bad as it appears at first sight. To determine how sensitive the PK results are to changes in individual rate constants, we have solved the differential equations for several values of a given rate constant $k_i$ while keeping the other rate constants fixed. We have found that under the gas-phase conditions mentioned above the TOF is rather insensitive to changes in $k_6$, $k_7$, and $k_9$, and it is more sensitive to the value of $k_8$. Therefore, large differences between the optimized values of $k_6$, $k_7$, and $k_9$ and the correct values do not affect the TOF much. This means that even if the PK theory was correct for this particular system, it would be difficult to determine the constants $k_6$, $k_7$, and $k_9$ accurately by fitting because both the accuracy of the measurements of the TOF and that of the optimization procedure would have to be extremely high.

TABLE IV. Reaction rate constants $k_i$ $(i=6,7,8,9)$ for the four reaction mechanisms. $k_{\mathrm{kMC}}$ are the rate constants used in the kMC simulations (Table I). $k_{\mathrm{fit}\_t}$ are the rate constants obtained by fitting the PK TOFs to the time evolution of the kMC TOFs [Fig. 6(a)]. $k_{\mathrm{fit}\_p}$ are the rate constants obtained by fitting the steady-state PK TOFs to the partial pressure dependence of the kMc TOFs [Fig. 6(b)]. Two sets of gas-phase conditions are considered for the fitting of $k_{\mathrm{fit}\_t}$, corresponding to the peak catalytic activity in Figs. 4(b) and 5(b): $T=350$ K, $p_{\mathrm{CO}}=4\times10^{-10}$ atm, and $p_{\mathrm{O}_2}=1\times10^{-10}$ atm and $T=600$ K, $p_{\mathrm{CO}}=7$ atm, and $p_{\mathrm{O}_2}=1$ atm. For the fitting of $k_{\mathrm{fit}\_p}$ the partial pressure $p_{\mathrm{CO}}$ was varied for fixed $T=600$ K and $p_{\mathrm{O}_2}=1$ atm.

| Reaction mechanism | $k_{\mathrm{kMC}}$(350 K) | $k_{\mathrm{fit}\_t}$ | $k_{\mathrm{kMC}}$(600 K) | $k_{\mathrm{fit}\_t}$ | $k_{\mathrm{fit}\_p}$ |
|---|---|---|---|---|---|
| $\mathrm{CO^{br}+O^{cus}} \xrightarrow{k_6} \mathrm{CO_2}$ | 11 | $1.8\times10^{-3}$ | $1.2\times10^{6}$ | $1.3\times10^{6}$ | $1.0\times10^{4}$ |
| $\mathrm{CO^{br}+O^{br}} \xrightarrow{k_7} \mathrm{CO_2}$ | $9.2\times10^{-10}$ | $9.2\times10^{-5}$ | 1.6 | $1.3\times10^{6}$ | $3.0\times10^{4}$ |
| $\mathrm{CO^{cus}+O^{cus}} \xrightarrow{k_8} \mathrm{CO_2}$ | 0.4 | 22 | $1.7\times10^{5}$ | $1.5\times10^{6}$ | $4.4\times10^{3}$ |
| $\mathrm{CO^{cus}+O^{br}} \xrightarrow{k_9} \mathrm{CO_2}$ | $1.9\times10^{-5}$ | 0.15 | $5.2\times10^{2}$ | $5.2\times10^{5}$ | $3.4\times10^{3}$ |

This situation is not unusual in phenomenological kinetics where it often happens that one cannot obtain precise information about the rate of some of the reactions in an overall mechanism. On the other hand, the fact that the value of $k_8$ giving the best fit differs from the correct one by an order of magnitude is significant and indicates that the phenomenological theory is deficient.

The fit reported above is the best we have obtained. The same type of study for $T=600$ K, $p_{\mathrm{CO}}=7$ atm, and $p_{\mathrm{O}_2}=1$ atm results in more serious discrepancies. The best fit to the data is poor (not shown), and the rate constants giving the best fit are shown in Table IV, where the column $k_{\mathrm{kMC}}$(600 K) gives the rate constants used in kMC and $k_{\mathrm{fit}\_t}$ gives the rates obtained by the best fit. The two sets or rate constants are again quite different.

The reaction at 600 K and the pressures indicated above is very fast, and had we performed real experiments we would have not been able to measure the evolution of TOF in time. A fit of the dependence of the steady-state TOF on the gas-phase conditions (partial pressures and temperature) would be closer to what one would do in a real experiment. Such a fitting minimizes the error

$$e(k_6,k_7,k_8,k_9)=\sum_{\alpha=1}^{N}\{R_{\mathrm{kMC}}(p_\alpha,\infty) - R_{\mathrm{PK}}(p_\alpha,\infty,k_6,k_7,k_8,k_9)\}^2, \tag{20}$$

where $R_{\mathrm{kMC}}(p_\alpha,\infty)$ is the steady-state TOF for $CO_2$ formation obtained by kMC. Here, we illustrate this by fixing $T=600$ K and $p_{\mathrm{O}_2}=1$ atm and by varying the CO partial pressure $p_\alpha=p_{\mathrm{CO}}$. $R_{\mathrm{PK}}(p_\alpha,\infty,k_6,k_7,k_8,k_9)$ is the turnover frequency calculated with the PK theory under the conditions used to obtain $\mathrm{R_{kMC}}$; $k_6$, $k_7$, $k_8$, and $k_9$ are adjustable and the other rate constants are held fixed at the values used in kMC. The infinity symbol in the above equation indicates that we use the steady-state TOF.

In Fig. 6(b) we show the dependence of the TOF on $p_{\mathrm{CO}}$ obtained in the kMC simulation, in the PK calculations with the kMC rate constants, as well as in the PK calculations using the values of $k_6$, $k_7$, $k_8$, and $k_9$ that give the best fit. The fit is poor. The rate constants giving the best fit are shown in column $k_{\mathrm{fit}\_p}$ of Table IV, and they should be compared to the values shown in column $k_{\mathrm{kMC}}$(600 K). The values produced by the best fit are very different from the correct ones (i.e., the values used in kMC).

A qualitative, partial understanding of the reasons for the poor fit is obtained by studying numerically the behavior of the system at low and high pressures. We find that rate constants that fit the low pressure data are very different from those that fit the high pressure data. This is because the shape of the TOF curve versus the CO pressure, given by PK, has a different character than that observed in kMC, and the PK equations are apparently unable to reproduce the steep rise in the kMC TOF curve when approaching the highest activity state from the low pressure side.

Our conclusion is that even though this is a relatively simple system, the phenomenological theory fails to represent the experimental result. Even worse, it could be misleading and could give a good fit to the data and erroneous rate constants.

## V. WHAT IS THE SOURCE OF ERROR IN THE PHENOMENOLOGICAL THEORY?

As we discussed in Sec. II a major approximation made by phenomenological kinetics is the replacement of the number of pairs that are in position to react with the mean-field approximation indicated in Eq. (18). For the reaction $\mathrm{CO^{cus}+O^{br}}$ the general notation [Eq. (18)] becomes

$$N_2(\mathrm{CO^{cus}},\mathrm{O^{br}}) \to \frac{N}{2}\frac{N_1(\mathrm{CO^{cus}})}{N^{\mathrm{cus}}}\frac{N_1(\mathrm{O^{br}})}{N^{\mathrm{br}}} = 2\frac{N_1(\mathrm{CO^{cus}})N_1(\mathrm{O^{br}})}{N} = \frac{N}{2}\theta\mathrm{CO^{cus}}\theta\mathrm{O^{br}}. \tag{21}$$

$N_2(\mathrm{CO^{cus}},\mathrm{O^{br}})$ is the number of CO molecules in a cus site that have an O atom in a nearest-neighbor br site; $N_1(\mathrm{O^{br}})$ is the number of oxygen atoms in a br site; $N_1(\mathrm{CO^{cus}})$ is the number of CO molecules in a cus site; $N$ is the total number of sites (br+cus) in the lattice. The PK theory assumes that the left-hand side of Eq. (21) is equal to the right-hand side. Similar assumptions are made for the reactions $\mathrm{CO^{cus}+O^{cus}}$,

TABLE V. $N_2(A^x,B^y)$ is the average number of A-B pairs that are nearest neighbors with A in site $x$ and B in site $y$ (A and B could be O or CO, and $x$ and $y$ could be the br or cus sites). $N_1(A^x)$ is the average number of A species at site $x$, and $N$ is the total number of sites on the surface. If there are no correlations in the occupation of the lattice sites, the values of $N_2/N$ and $2N_1N_1/N^2$ provided by kMC would be equal for each pair of species. We also give the values of $\frac{1}{2}\theta\theta$ as obtained by PK, where $\theta=N_1/N^x$. Again, if PK (based on the mean-field approximation and neglecting the detailed lattice structure) was correct, $\frac{1}{2}\theta\theta$ should be equal to $2N_1N_1/N^2$. The two sets of gas-phase conditions for which this analysis is performed correspond to the peak catalytic activity in Figs. 4(b) and 5(b): $T=350$ K, $p_{CO}=4\times10^{-10}$ atm, and $p_{O_2}=1\times10^{-10}$ atm and $T=600$ K, $p_{CO}=7$ atm, and $p_{O_2}=1$ atm. We examine the reaction system after it reached a steady state.

| | $T$ K | | $CO^{cus}-O^{cus}$ | $CO^{br}-O^{br}$ | $CO^{br}-O^{cus}$ | $CO^{cus}-O^{br}$ |
|---|---|---|---|---|---|---|
| kMC | 600 | $N_2/N$ | 0.11 | 0.063 | 0.0023 | 0.68 |
| kMC | 600 | $2N_1N_1/N^2$ | 0.10 | 0.028 | 0.0078 | 0.34 |
| PK | 600 | $\frac{1}{2}\theta\theta$ | 0.024 | 0.10 | 0.019 | 0.13 |
| kMC | 350 | $N_2/N$ | 0.010 | 0.0050 | 0.000001 | 0.42 |
| kMC | 350 | $2N_1N_1/N^2$ | 0.035 | 0.0025 | 0.00020 | 0.23 |
| PK | 350 | $\frac{1}{2}\theta\theta$ | 0.009 | 0.0002 | 0.000006 | 0.30 |

$CO^{br}+O^{cus}$, and $CO^{br}+O^{br}$ and for the adsorption and desorption of $O_2$.

The validity of this approximation can be tested because the kMC simulations calculate exactly the quantities $N_2(A^x,B^y)$, $N_1(A^x)$, and $N_1(B^x)$ for all species, at all sites, and at all times during the evolution of the system. In Table V we give the average values of $N_2(A^x,B^y)/N$ and $2N_1(A^x)N_1(B^y)/N^2$ evaluated during the steady state for the gas-phase conditions that correspond to the peak catalytic activity at $T=600$ K ($p_{CO}=7$ atm and $p_{O_2}=1$ atm), and we compare them to the values of $\frac{1}{2}\theta(A^x)\theta(B^y)$ that result from the PK simulations under the same gas-phase conditions. If there were no correlations in the site occupations, then $N_2(A^x,B^y)/N$ and $2N_1(A^x)N_1(B^y)/N^2$ would be equal in the kMC simulations. In addition, if the PK (based on the mean-field assumption and not accounting for the detailed lattice structure) gave a perfect description of the kinetics, then $N_2(A^x,B^y)/N$ would be equal to $\frac{1}{2}\theta(A^x)\theta(B^y)$, where the coverages $\theta$ are calculated by solving the PK differential equations. Table V demonstrates clearly that this equality is not found in the simulation.

The correlations in the site occupations accounted for in the kMC simulations suppress, in particular, the $CO^{br}+O^{cus}$ pairs compared to a random arrangement on the lattice (0.0023 vs 0.0078 at 600 K, Table V). This is illustrated in Fig. 7, which shows a snapshot of the occupation of the lattice at the steady state at these gas-phase conditions. Almost all $CO^{br}$ species are chaperoned by $CO^{cus}$ molecules in the neighboring cus sites. Due to the lack of suitable neighboring pairs, this further suppresses the $CO^{br}+O^{cus}$ reaction despite its most favorable rate constant among the four possible reaction mechanisms. We note that it is interesting to see that even though there are no lateral interactions between the adsorbed species in the kMC model, the chemical reactions manage to create a fair degree of aggregation (regions having concentrations substantially higher or lower than the average concentration) in spite of the fact that diffusion is included in the simulation. This structure is primarily created by the fact that $O_2$ adsorption requires two sites and a CO one, and because the creation of the vacant sites by desorption and reactions is structure dependent.

## VI. CONCLUSIONS

The comparison of the phenomenological equations to kMC simulation has the advantage that in kMC we know the rate constants, the reaction mechanism, and the structure of the surface. Therefore, any discrepancy between the two methods is due to intrinsic shortcomings of the phenomenological theory. The model examined here has not been designed to create difficulties for the phenomenological theory. Surface diffusion is taken into account, and the deposition of the molecules on the surface is made at random. In addition, there are no lateral interactions in the model that would create a thermodynamic driving force towards the appearance of domains having different reactant concentrations. Therefore, in principle, the reactants can mix well, making the assumptions underlying PK theory more likely to be correct. Nevertheless, we find that the PK equations describe the kinetics poorly. When used with the correct rate constants, PK fails to find which reaction is dominant, gives poor results for the

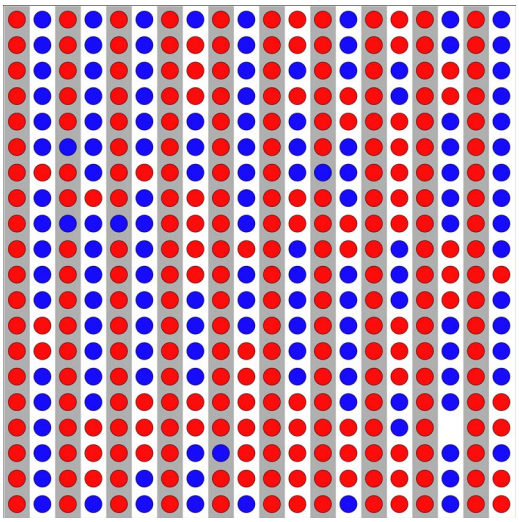

FIG. 7. (Color online) Snapshot of the steady-state surface population under optimum catalytic conditions at 600 K ($p_{O_2}=1$ atm and $p_{CO}=7$ atm). Shown is a schematic top view of the simulation area of $20\times20$ surface sites, where the substrate bridge sites are marked by gray stripes and the cus sites by white stripes. Oxygen atoms are drawn as red circles and the adsorbed CO molecules as blue circles.

rates, and does not predict the best reaction conditions correctly. Moreover, when we use the PK equations to fit the "data" provided by kMC, we obtain a good fit but poor rate constants in one example, and a poor fit and poor rate constants in the others. Moreover, the errors in PK are largest at the pressures and temperatures most relevant to commercial catalysts.

The PK theory assumes that the number of pairs $N_2(A^x,B^y)$ of molecules A and B, located next to each other in the sites $x$ and $y$, can be approximated by $2N_1(A^x)N_1(B^y)/N$. The kMC simulations allow the determination of $N_2(A^x,B^y)$, $N_1(A^x)$, and $N_1(B^y)$ at all times during the reaction. By monitoring these quantities during a simulation we find that $N_2(A^x,B^y)$ differs from $2N_1(A^x)N_1(B^y)/N$, which means that the right-hand side of the rate equations [Eqs. (10)–(13)] is erroneous. This error has a cumulative effect when the differential equations are integrated and can lead to substantial errors in the TOF.

Replacing $N_2(A^x,B^y)$ with $2N_1(A^x)N_1(B^y)/N$ is a typical mean-field approximation. It neglects fluctuations in composition even though they are unavoidable (the number of nearest neighbors of a specific species is not equal to the mean number of neighbors). In addition, some systems have a propensity to aggregate creating domains rich in A and domains rich in B. This usually happens when the A-A interactions and the B-B interactions exceed the A-B ones and when the temperature is not very high. Finally, large differences in binding energies can also lead to segregation on lattices with different types of sites: for example, if O binds to the br sites much more strongly than to the cus sites and if CO binds weakly to the br sites, we expect to have an excess of O atoms in the br sites rather than a random distribution of O and CO.

The magnitudes of the binding energies and of the adsorbate-adsorbate interaction energies affect the equilibrium properties of the system. However, in most kinetic studies the system is kept out of equilibrium. In our model this is done by supplying $O_2$ and CO to keep their partial pressure constant and by removing $CO_2$ from the surface. These conditions counteract the natural tendency of the system to evolve towards equilibrium and can be an additional source of segregation. For example, oxygen accumulates in the br sites because once adsorbed it is slow to desorb or to react with CO, while CO disappears rapidly from the bridge sites because its desorption is fast and so is the reaction $CO^{br}+O^{cus}\rightarrow CO_2$.

While we show that phenomenological kinetics has shortcomings when used to describe catalytic reactions, it might be useful when used with proper skepticism. If the equations fit the data, they can be used in a reactor design as long as one does not extrapolate them too far from the conditions under which the data were taken. If the segregation of the reactants is not dramatic, the PK equations may provide some useful insights. For the model studied here they capture the general form of the "kinetic phase diagram" and the fact that the dependence of TOF on partial pressure has a sharp peak. This knowledge is useful since it informs us that we cannot decide that a catalyst (Ru in our case) performs poorly if we have studied the kinetics only for a limited number of partial pressures. Unfortunately, we have no *a priori* criterion to decide which results of PK can be trusted.

## ACKNOWLEDGMENTS

The authors gratefully acknowledge the support of the work done in Santa Barbara by the Air Force Office for Scientific Research. The work done in Berlin was partially supported by the Deutsche Forschungsgemeinschaft (SPP 1091) and the EU STREP program $NanO_2$. One of the authors (H.M.) acknowledges support by the Alexander von Humboldt Foundation. Sebastian Matera is thanked for critical discussions on the mean-field modeling and for a careful reading of the manuscript.

## APPENDIX

The adsorption rate constants ($k_i$'s) employed in the model are given by

$$k_i = \frac{p_A A_s}{\sqrt{2\pi m_A k_B T}}, \quad i = 1,2,\ldots,5, \tag{A1}$$

where $A_s$ is the area of a site, and the desorption rate constants are

$$k_{-i} = k_i \exp\left(\frac{E_i + \mu_A}{k_B T}\right), \quad i = 1,2,\ldots,5. \tag{A2}$$

Here, $i=1,2,\ldots,5$ labels the reaction, $k_i$ is the forward rate constant, and $k_{-i}$ is the backward rate constant. A labels the species (i.e., $O_2$ or CO), and $p_A$, $m_A$, and $\mu_A$ are the partial pressure, the mass, and the chemical potential, respectively, of species A. The gas-phase chemical potential is calculated by assuming that the gas is an ideal mixture and by making the harmonic oscillator and rigid rotor approximations.[56] $E_i$ are the energy barriers to desorption calculated by density-functional theory.[23]

The reaction rates are calculated from

$$k_i = \frac{1}{2}\frac{k_B T}{h}\exp\left(\frac{-E_i}{k_B T}\right), \quad i = 6,7,8,9. \tag{A3}$$

Since the hopping rates leading to diffusion are not taken into account in the PK equations, we do not give them here. They can be found in Ref. 23.

The kMC rate constants have been calculated with Eqs. (A1)–(A3) and using the activation energies given in Eqs. (1)–(9). In Table I we list the numerical values for the two $(T,p)$ conditions mainly discussed in the text.

[1] A. B. Bortz, M. H. Kalos, and J. L. Lebowitz, J. Comput. Phys. **17**, 10 (1975).
[2] K. A. Fichthorn and W. H. Weinberg, J. Chem. Phys. **95**, 1090 (1991).
[3] P. A. Maksym, Semicond. Sci. Technol. **3**, 594 (1988).
[4] A. F. Voter, Phys. Rev. B **34**, 6819 (1986).
[5] V. P. Zhdanov, Surf. Sci. **500**, 966 (2002).
[6] R. M. Ziff, E. Gulari, and Y. Barshad, Phys. Rev. Lett. **56**, 2553 (1986); B. J. Brosilow and R. M. Ziff, Phys. Rev. A **46**, 4534 (1992).
[7] G. M. Buendia, E. Machado, and P. A. Rikvold, J. Mol. Struct.: THEOCHEM **769**, 189 (2006).
[8] D. J. Liu and J. W. Evans, J. Chem. Phys. **117**, 7319 (2002).
[9] D. J. Liu and J. W. Evans, Multiscale Model. Simul. **4**, 424 (2005).
[10] D. J. Liu and J. W. Evans, J. Chem. Phys. **124**, 154705 (2006).
[11] F. J. Gracia and E. E. Wolf, Chem. Eng. Sci. **59**, 4723 (2004).

[12] E. Machado, G. M. Buendia, P. A. Rikvold, and R. M. Ziff, Phys. Rev. E **71**, 016120 (2005).
[13] N. V. Petrova and I. N. Yakovkin, Surf. Sci. **578**, 162 (2005).
[14] A. Provata and V. K. Noussiou, Phys. Rev. E **72**, 066108 (2005).
[15] D. Y. Hua and Y. Q. Ma, Phys. Rev. E **66**, 066103 (2002).
[16] D. Y. Hua, S. J. Shao, and S. Lin, Phys. Rev. E **69**, 046114 (2004).
[17] R. H. Goodman, D. S. Graff, L. M. Sander, P. LerouxHugon, and E. Clement, Phys. Rev. E **52**, 5904 (1995).
[18] N. Pavlenko, J. W. Evans, D. J. Liu, and R. Imbihl, Phys. Rev. E **65**, 016121 (2002).
[19] Y. Suchorski, J. Beben, R. Imbihl, E. W. James, D. J. Liu, and J. W. Evans, Phys. Rev. B **63**, 165417 (2001).
[20] E. Clement, P. LerouxHugon, and L. M. Sander, Phys. Rev. E **52**, 5997 (1995).
[21] K. Reuter, D. Frenkel, and M. Scheffler, Phys. Rev. Lett. **93**, 116105 (2004).
[22] K. Reuter and M. Scheffler, Phys. Rev. Lett. **90**, 046103 (2003).
[23] K. Reuter and M. Scheffler, Phys. Rev. B **73**, 045433 (2006).
[24] G. F. Froment, Catal. Rev. - Sci. Eng. **47**, 83 (2005).
[25] E. Kotomin and V. Kuzovkov, in *Comprehensive Chemical Kinetics*, edited by R. G. Compton and G. Hancock (Elsevier, Amsterdam, 1996), Vol. 34, p. 1.
[26] J. M. White, in *Comprehensive Chemical Kinetics*, edited by C. H. Bamford and C. F. H. Tipper (Elsevier, Amsterdam, 1972), Vol. 6, p. 201.
[27] H. Metiu, *Physical Chemistry: Thermodynamics*, 1st ed. (Taylor & Francis, London, 2006), Vol. 1.
[28] R. K. Boyd, Chem. Rev. (Washington, D.C.) **77**, 93 (1977).
[29] K. Denbigh, *The Principles of Chemical Equilibrium* (Cambridge University Press, Cambridge, 1993).
[30] E. Clement, P. Lerouxhugon, L. M. Sander, and P. Argyrakis, J. Phys. Chem. **98**, 7274 (1994).
[31] R. Dickman, Phys. Rev. A **34**, 4246 (1986).
[32] J. W. Evans, D. J. Liu, and M. Tammaro, Chaos **12**, 131 (2002).
[33] J. Wang, C. Y. Fan, K. Jacobi, and G. Ertl, Surf. Sci. **481**, 113 (2001).
[34] K. Reuter, M. V. Ganduglia-Pirovano, C. Stampfl, and M. Scheffler, Phys. Rev. B **65**, 165403 (2002).
[35] K. Reuter and M. Scheffler, Surf. Sci. **490**, 20 (2001).
[36] K. Reuter and M. Scheffler, Phys. Rev. B **65**, 035406 (2001).
[37] K. Reuter and M. Scheffler, Phys. Rev. B **68**, 045407 (2003).
[38] K. Reuter, C. Stampfl, M. V. Ganduglia-Pirovano, and M. Scheffler, Chem. Phys. Lett. **352**, 311 (2002).
[39] J. Assmann, V. Narkhede, L. Khodeir, E. Loffler, O. Hinrichsen, A. Birkner, H. Over, and M. Muhler, J. Phys. Chem. B **108**, 14634 (2004).
[40] V. Narkhede, J. Assmann, and M. Muhler, Z. Phys. Chem. **219**, 979 (2005).
[41] Y. D. Kim, H. Over, G. Krabbes, and G. Ertl, Top. Catal. **14**, 95 (2001).
[42] Y. D. Kim, A. P. Seitsonen, and H. Over, Surf. Sci. **465**, 1 (2000).
[43] Y. D. Kim, A. P. Seitsonen, and H. Over, Phys. Rev. B **63**, 115419 (2001).
[44] Y. D. Kim, A. P. Seitsonen, S. Wendt, J. Wang, C. Fan, K. Jacobi, H. Over, and G. Ertl, J. Phys. Chem. B **105**, 3752 (2001).
[45] H. Madhavaram, H. Idriss, S. Wendt, Y. D. Kim, M. Knapp, H. Over, J. Assmann, E. Loffler, and M. Muhler, J. Catal. **202**, 296 (2001).
[46] H. Over, Y. D. Kim, A. P. Seitsonen, S. Wendt, E. Lundgren, M. Schmid, P. Varga, A. Morgante, and G. Ertl, Science **287**, 1474 (2000).
[47] H. Over and M. Muhler, Prog. Surf. Sci. **72**, 3 (2003).
[48] H. Over, A. P. Seitsonen, E. Lundgren, M. Schmid, and P. Varga, J. Am. Chem. Soc. **123**, 11807 (2001).
[49] H. Over, A. P. Seitsonen, E. Lundgren, M. Schmid, and P. Varga, Surf. Sci. **515**, 143 (2002).
[50] H. Over, A. P. Seitsonen, E. Lundgren, M. Smedh, and J. N. Andersen, Surf. Sci. **504**, L196 (2002).
[51] K. Reuter and M. Scheffler, Appl. Phys. A: Mater. Sci. Process. **78**, 793 (2004).
[52] A. P. Seitsonen, Y. D. Kim, M. Knapp, S. Wendt, and H. Over, Phys. Rev. B **65**, 035413 (2002).
[53] S. Wendt, M. Knapp, and H. Over, J. Am. Chem. Soc. **126**, 1537 (2004).
[54] S. Wendt, A. P. Seitsonen, Y. D. Kim, M. Knapp, H. Idriss, and H. Over, Surf. Sci. **505**, 137 (2002).
[55] S. Wendt, A. P. Seitsonen, and H. Over, Catal. Today **85**, 167 (2003).
[56] D. A. McQuarrie, *Statistical Mechanics*, 2nd ed. (University Science Books, Sausalito, 2000).